

Influence of Nanofiller Dimensionality on the Crystallization Behavior of HDPE/Carbon Nanocomposites

Xiaomei Shi, Jingdai Wang, Binbo Jiang, Yongrong Yang

State Key Laboratory of Chemical Engineering, Department of Chemical and Biological Engineering, Zhejiang University, Hangzhou 310027, People's Republic of China

Correspondence to: J. Wang (E-mail: wangjd@zju.edu.cn)

ABSTRACT: The isothermal and nonisothermal crystallization behavior of high density polyethylene (HDPE) containing various zero, one, and two dimensional (0-D, 1-D, and 2-D) carbon nanofillers were investigated by means of differential scanning calorimetry. For a given temperature, the isothermal crystallization incubation time of HDPE became longer with the addition of lower dimensional carbon nanofillers, and the isothermal crystallization rate got slower. The values of Avrami and Tobin exponents indicated that the isothermal crystallization of HDPE followed two-dimensional crystal growth in the presence of 2-D and 1-D carbon nanofillers, while exhibited three-dimensional heterogeneous crystal growth in the presence of 0-D carbon nanofillers. Contrary to the isothermal study, the nonisothermal crystallization of HDPE was accelerated in the presence of lower dimensional nanofillers. The nonisothermal crystallization data were finally analyzed using Ozawa and Mo methods. It was observed that only Mo approach could successfully describe the nonisothermal crystallization process of HDPE and HDPE/carbon nanocomposites. © 2012 Wiley Periodicals, Inc. *J. Appl. Polym. Sci.* 128: 3609–3618, 2013

KEYWORDS: crystallization; composites; differential scanning calorimetry; polyolefins

Received 28 May 2012; accepted 11 September 2012; published online 30 September 2012

DOI: 10.1002/app.38581

INTRODUCTION

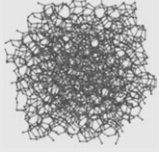
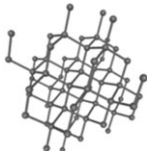
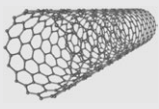

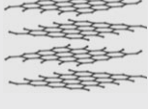
Polymer nanocomposites are particle-filled polymers for which at least one dimension of the dispersed particles is in the nanometer size range.¹ In virtue of the nanometer-size fillers, these polymer nanocomposites exhibit prominently improved mechanical, thermal, optical, and physic-chemical properties, comparing with the pure polymer or conventional filler-reinforced polymer composites.

The crystallization behavior of polymer matrix, which is of significant importance for real industrial processing, could also be influenced by the dispersed nanofillers and hence has aroused wide attention of researchers. It was found that the layered silicates,^{2–7} spherical silica,⁸ and calcium carbonate⁹ played two different roles during polymer crystallization: as heterogeneous nucleating agent which promoted polymer crystallization and as a hindrance which retarded polymer crystallization growth. Generally, these effects are dependent on the content, the geometry, and the dispersion state of the nanofillers in the polymer as well as the crystallization temperature.

Among the nanofillers involved in recent studies, carbon nanostructured material is a family which has received considerable attention,^{10–13} due to their outstanding mechanical, electrical,

thermal, and flame retardant properties. The entire range of dimensionalities is represented in the nanocarbon world,¹⁴ including zero-dimensional (0-D) structures (e.g., fullerenes, diamond clusters), one-dimensional (1-D) structures (e.g., carbon nanotubes), and two-dimensional (2-D) structures (e.g., graphite sheets). The crystallization behavior of polymer/carbon nanocomposites has also stimulated increasing research interests. It was found that the incorporation of single-walled carbon nanotube (SWNT) into polypropylene^{15–20} accelerated the nucleation and resulted in shorter crystallization time, the effect being more appreciable at low nanotube content (5%). The same phenomena were observed for polyethylene/SWNT nanocomposites fabricated via hot-coagulation method.²¹ The nucleation effect of multiwalled carbon nanotube (MWNT) on the crystallization of polymer was also reported. The crystallization rate of polymer, including polyethylene,^{22,23} polypropylene,^{24,25} polyamide 6,²⁶ polyamide 1010,²⁷ and poly(epsilon-caprolactone),²⁸ was increased with the addition of MWNT. Recently, Sui²⁹ reported that diamine-modified MWNT reduced the overall crystallization rate of polyamide 6 matrix despite the heterogeneous nucleation effect. Similar results were also observed for *in situ* polymerized high density polyethylene (HDPE)/MWNT nanocomposites,³⁰ *in situ* synthesized polyamide 6/foliated

Table I. Information of Various Carbon Nanofillers

Nanofillers	Characteristics	Supplier	Structure
CB	Particle diameter = 20 nm, specific surface area (SSA) = 890 m ² /g	Shandong Huaguang Chemical Co. Ltd.	
Diamond	Particle diameter = 3-10 nm, SSA = 270-335 m ² /g	Heyuan Zhonglian Nanotechnology Co. Ltd.	
SWNT	Diameter = 0.8-1.6 nm, length = 5-40 μm, SSA = 407 m ² /g	Chengdu Organic Chemical Co. Ltd.	
MWNT	Outer diameter < 8 nm, inner diameter = 2-5 nm, length = 10-30 μm, SSA > 500 m ² /g	Chengdu Organic Chemical Co. Ltd.	
Graphite	Layer thickness = 5-25 nm, lateral dimension = 0.5-20 μm, SSA = 40-60 m ² /g	Xiamen Knano Graphene Technology Co. Ltd.	

graphite nanocomposites,³¹ and polyamide 6/graphite oxide nanocomposites prepared by delamination/absorption.³² Apparently, particular attention has been paid to polymer/1-D carbon nanotube composites, whereas few studies have been devoted to the crystallization of polymer/0-D and polymer/2-D carbon nanocomposites.³³ Moreover, comprehensive study is also scarce to understand the influence of nanofiller dimensionality on the crystallization kinetics of polymer nanocomposites.

With the above considerations in mind, the crystallization behavior of HDPE containing various dimensional (0-D, 1-D, and 2-D) carbon nanofillers, was investigated using differential scanning calorimeter (DSC) under isothermal and nonisothermal conditions. Several theoretical models (Avrami, Tobin, Ozawa, and Mo) were applied to describe the crystallization process. The influence of the presence and the dimensionality of the carbon nanofillers on the crystallization kinetics of HDPE were discussed.

EXPERIMENTAL SECTION

Materials and Nanocomposite Preparation

Commercial HDPE ($\rho = 0.949 \text{ g/cm}^3$, melt flow index = 0.40 g/10 min) without additives was kindly supplied by SINOPEC Shanghai Petrochemical Co. Ltd. in the form of powder. The carbon nanofillers used in this study were 0-D carbon black (CB) and diamond, 1-D SWNT and MWNT, and 2-D foliated graphite. Detailed information of these carbon nanofillers is given in Table I.

The HDPE nanocomposites containing 2 wt % of each carbon nanofiller were prepared by melt-blending using a Bradender Plastic-Corder W50EHT internal mixer at 190°C, 60 rpm for 10 min. Square plaques were then prepared for further testing by compression-molding of the mixtures for 5 min at 180°C and 25 bar in a molding test press. Blank sample was obtained following the same procedures as a base of comparison.

Crystallization Study

The isothermal and nonisothermal crystallization study of HDPE/carbon nanocomposites were carried out on a Perkin-Elmer DSC-7 under nitrogen atmosphere. Sample of approximately 8 mg was used for each measurement. For isothermal crystallization, the samples were first heated from 30°C to 160°C at a rate of 50°C/min, and then stayed there for 5 min to erase any previous thermal history. After that, the samples were rapidly cooled to the designated crystallization temperature and kept at that temperature until the crystallization completed. To insure the integrity of the isothermal crystallization process and the reliability of the calculated kinetic data, proper temperatures for isothermal crystallization should be selected. For this reason, the isothermal crystallization measurements of each sample were carried out at a temperature range of 120°C to 125°C. Finally, the crystallization temperature of 122, 123, and 124°C were chosen for HDPE and HDPE/graphite nanocomposite; 121, 122, and 123°C were chosen for HDPE/SWNT and HDPE/MWNT nanocomposites; 120, 121, and 122°C were chosen for HDPE/CB and HDPE/diamond nanocomposites.

To examine nonisothermal crystallization, the samples were heated from 30°C to 180°C, held for 5 min and then cooled to 30°C at constant cooling rates of 5, 10, 15, and 20°C/min. The absolute crystallinity of HDPE is determined by the standard DSC scans: The samples were cooled from the melt (180°C) to 25°C at 10°C/min, holding there for 5 min, and then heated to 180°C at 10°C/min.

Description of Theoretical Models

To analyze the crystallization data obtained from DSC, several theoretical models (Avrami, Tobin, Ozawa and Mo) are used in this study.

Generally, the classical Avrami equation^{34,35} is used to analyze the isothermal crystallization kinetics of polymer materials:

$$X_t = 1 - \exp[-(K_a t)^{n_a}] \quad (1)$$

where X_t is the relative crystallinity at time t . n_a is the Avrami exponent, which reveals the nucleation mechanism and growth dimension, and K_a is the Avrami crystallization rate constant.

As Avrami analysis is only appropriate to describe the early stages of polymer crystallization, Tobin theory,³⁶ which involved phase-transformation kinetics with growth site impingement, was thus proposed to improve the fitting results at the later stages of crystallization:

$$X_t = \frac{(K_t t)^{n_t}}{1 + (K_t t)^{n_t}} \quad (2)$$

where K_t is the Tobin crystallization rate constant and n_t is the Tobin exponent governed by different types of nucleation and growth mechanisms.

Considering the nonisothermal character of the process, Ozawa³⁷ modified the Avrami equation by incorporating the cooling rate factor (Φ) based on the mathematical derivation of Evans.³⁸ The Ozawa equation is as follows:

$$1 - X_T = \exp[-K_T / \Phi^m] \quad (3)$$

where K_T and m are the Ozawa crystallization rate constant and exponent, respectively. Equation (3) can be written as the double logarithmic form:

$$\log[-\ln(1 - X_T)] = \log K_T - m \log \Phi \quad (4)$$

If Ozawa analysis is valid to describe the kinetics of nonisothermal crystallization, the plots of $\log[-\ln(1 - X_T)]$ against $\log \Phi$ should give a straight line, and the kinetic parameters m and K_T can be derived from the slope and the intercept, respectively.

Combining the Avrami equation with the Ozawa equation, a method modified by Mo and coworkers³⁹ was also proposed to describe the nonisothermal crystallization. The final modified equation is:

$$\log \Phi = \log F(T) - b \log t \quad (5)$$

where the parameter $F(T)$ refers to the value of cooling rate required to reach a certain degree of crystallinity at unit crystal-

lization time and b is the ratio between Avrami and Ozawa exponents, that is, $b = n/m$. Thus, plotting $\log \phi$ versus $\log t$ at a given relative crystallinity yields a linear relationship between $\log \phi$ and $\log t$. The values of b and $F(T)$ can be estimated from the slope and the intercept of the line.

RESULTS AND DISCUSSION

Isothermal Crystallization Analysis

Isothermal Crystallization Behavior. The typical isothermal crystallization curves of HDPE and HDPE/carbon nanocomposites at different crystallization temperatures (T_c) are shown in Figure 1. The crystallization behavior of the samples is strongly affected by T_c . With the T_c increased, the crystallization exothermic peaks become flatter and shift to a higher value, meanwhile the time to complete crystallization is also increased. The relative crystallinity at time t (X_t) can be obtained from the area under the exotherm up to time t , divided by the total exothermic peak area:

$$X_t = \frac{\int_0^t \frac{dH_c}{dt} \cdot dt}{\int_0^\infty \frac{dH_c}{dt} \cdot dt} \quad (6)$$

where dH_c is the enthalpy of crystallization released during an infinitesimal time interval dt . Thus the development of X_t with crystallization time for HDPE and HDPE/carbon nanocomposites can be established as shown in Figure 2. The half time of crystallization $t_{1/2}$, at which $X_t = 0.5$, can be determined from these curves. The intersection of the time axis with the tangent at the inflection point of the curve defines the incubation time, t_i . Generally, $t_{1/2}$ of a polymer is taken as a measure of the overall rate of crystallization, and t_i is the time required before the critical equilibrium nucleus dimension is established.⁴⁰ The values of both $t_{1/2}$ and t_i for isothermal crystallization of HDPE and the nanocomposites are listed in Table II. It can be seen that $t_{1/2}$ and t_i of all samples increase with increasing T_c . The increased $t_{1/2}$ indicates that the crystallization rate decreases with increasing T_c , which verifies that the crystallization takes place by a nucleation-controlled mechanism. Meanwhile, the increased t_i suggests that longer time is needed to reach the critical equilibrium nucleus dimension under higher T_c . On the other hand, for a given T_c , both $t_{1/2}$ and t_i increase progressively with the addition of SWNT, MWNT, CB, and diamond, whereas decreased slightly with the addition of graphite. That is, the 1-D (SWNT and MWNT) and 0-D (CB and diamond) carbon nanofillers decelerate the isothermal crystallization process of HDPE. This could be attributed to the small dimension and steric effect of the carbon nanofillers. The lower dimensionality the carbon nanofiller has, the longer incubation time it needs for the polymer to reach the critical equilibrium nucleus dimension. For HDPE/graphite nanocomposites, the continuum plane of relatively large graphite sheet can easily absorb the HDPE chains and lead HDPE to crystallize, hence, less incubation time is needed and the crystallization is slightly promoted.

The Avrami and Tobin Methods. To analyze the isothermal crystallization kinetics, Avrami equation is firstly used. The values of K_a and n_a can be obtained by fitting X_t to eq. (1). The fitting profiles are presented in Figure 3(a). It is observed that

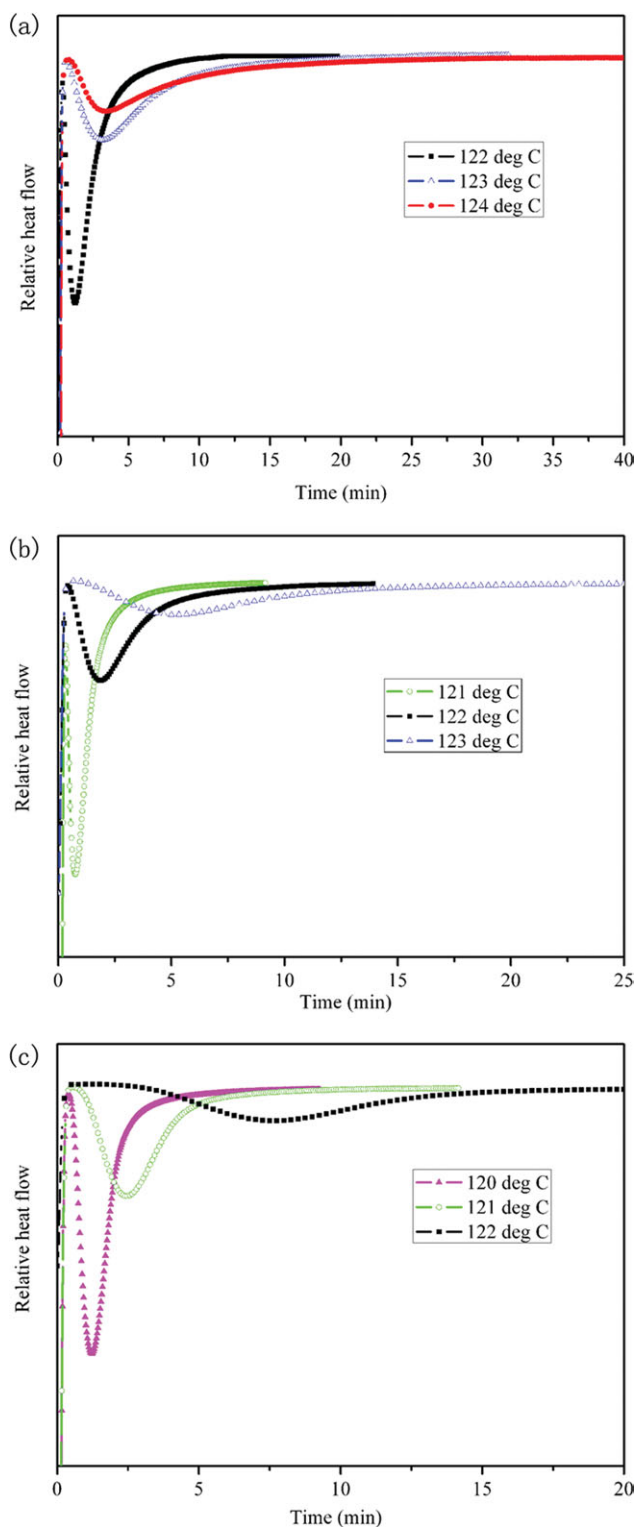


Figure 1. DSC curves of isothermal crystallization of HDPE and HDPE/carbon nanocomposites at different crystallization temperatures: (a) HDPE/Graphite; (b) HDPE/SWNT; (c) HDPE/CB. [Color figure can be viewed in the online issue, which is available at wileyonlinelibrary.com.]

there is a good consistency between the data and the model when X_t is below 0.80. The derivation of Avrami plot at the later stage of crystallization has also been found by Huang⁹ in

the isothermal crystallization behavior of HDPE/calcium carbonate composites, which may be attributed to the impinging effect. To improve the fitting results at the later stages of crystallization, Tobin analysis is hence introduced. The parameters K_t and n_t can also be estimated by fitting X_t to eq. (2). The fitting

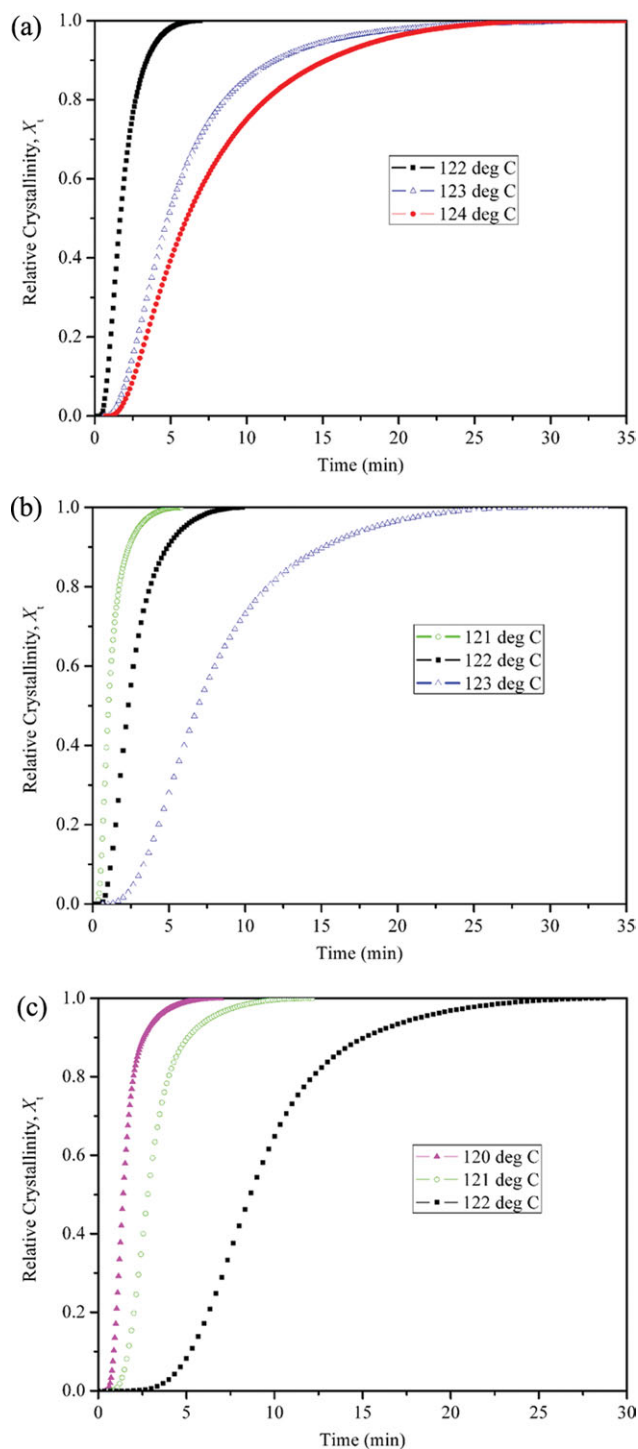


Figure 2. Development of relative crystallinity (X_t) with crystallization time for isothermal crystallization of (a) HDPE/Graphite; (b) HDPE/SWNT; (c) HDPE/CB. [Color figure can be viewed in the online issue, which is available at wileyonlinelibrary.com.]

Table II. Kinetic Parameters of Avrami and Tobin Models

T_c (°C)	Avrami			Tobin			t_i	$t_{1/2}$
	K_a (min ⁻¹)	n_a	R^2	K_t (min ⁻¹)	n_t	R^2		
HDPE								
122	0.462	1.87	0.9965	0.571	2.98	0.9989	0.68	1.75
123	0.166	1.50	0.9967	0.183	2.28	0.9971	1.60	5.37
124	0.099	2.21	0.9913	0.107	2.43	0.9952	3.29	7.44
HDPE/Graphite								
122	0.492	1.98	0.9974	0.595	3.12	0.9990	0.63	1.68
123	0.188	1.65	0.9985	0.206	2.49	0.9993	1.55	4.80
124	0.156	2.22	0.9970	0.163	2.49	0.9969	1.76	6.06
HDPE/SWNT								
121	0.776	1.89	0.9905	0.935	2.94	0.9983	0.45	1.05
122	0.354	1.98	0.9961	0.425	3.11	0.9992	0.98	2.33
123	0.125	2.06	0.9974	0.144	2.91	0.9995	2.54	6.93
HDPE/MWNT								
121	0.674	1.94	0.9914	0.806	3.01	0.9983	0.54	1.21
122	0.294	2.12	0.9974	0.346	3.31	0.9992	1.21	2.88
123	0.133	2.52	0.9985	0.151	3.26	0.9997	2.80	6.65
HDPE/CB								
120	0.616	2.70	0.9928	0.702	3.99	0.9985	0.81	1.41
121	0.316	2.65	0.9963	0.353	3.95	0.9993	1.42	2.81
122	0.103	3.11	0.9970	0.116	4.34	0.9998	4.53	8.65
HDPE/Diamond								
120	0.553	2.33	0.9862	0.641	3.39	0.9953	0.84	1.52
121	0.283	2.78	0.9938	0.320	4.16	0.9969	1.75	3.09
122	0.108	2.72	0.9949	0.121	4.39	0.9998	4.46	8.23

profiles are presented in Figure 3(b). It is obvious that Tobin equation is more effective than Avrami equation.

The values of K obtained from Avrami and Tobin models are summarized in Table II. As expected, the crystallization rate constant K of HDPE varies with the addition of different kinds of carbon nanofillers. For each sample, the value of K decreases with increasing T_c . For a given T_c studied here, the values of K are in the following order: HDPE/graphite \sim HDPE > HDPE/SWNT \sim HDPE/MWNT > HDPE/CB \sim HDPE/diamond. As higher K is always corresponding to lower $t_{1/2}$, suggesting faster crystallization, the values of K here are in accordance with the results discussed above. That means, the isothermal crystallization rate of HDPE keeps constant (or increases slightly) with the addition of 2-D carbon nanofiller (graphite), while decreases successively with 1-D (SWNT and MWNT) and 0-D (CB and diamond) carbon nanofillers.

The values of n for Avrami and Tobin models are also obtained and listed in Table II. The average value of n_a is close to 2 for pure HDPE. With the addition of graphite, SWNT, or MWNT, the value of n_a is only slightly higher and remains close to 2, indicating the simultaneous occurrence of two-dimensional crystal growths with heterogeneous nucleation.⁹ The n_a values of HDPE/CB and HDPE/diamond nanocomposites are much

higher than that of pure HDPE and are close to 3, implying a crystallization process with three-dimensional heterogeneous crystal growth.^{18,24} The value of n_t generally approximately to $n_a + 1$,³⁹ also increases successively for HDPE with 2-D, 1-D, and 0-D carbon nanofillers, ranging from 2.49 to 4.39. The increased n_a and n_t could be attributed to a change from instantaneous nucleation to sporadic nucleation. It seems that the crystallization of HDPE follows the two-dimensional lamellar crystal growths in the presence of 1-D or 2-D carbon nanofillers, while shows the three-dimensional spherical crystal growth with heterogeneous nucleation in the presence of 0-D carbon nanofillers. The schematic diagram of crystal growth of HDPE in the presence of various dimensional carbon nanofillers is proposed in Figure 4. In the presence of graphite or nanotubes, the HDPE chains firstly root on the surface of graphite sheet or nanotubes and then crystallize along the surface, similarly to that of HDPE/MWNT composites described by Kim.³⁰ While with the addition of 0-D carbon nanofillers, the crystallites prefer to grow in all directions and form the spherulites.

Nonisothermal Crystallization Analysis

Nonisothermal Crystallization Behavior. Standard DSC scans were recorded to determine the absolute crystallinity (X_c) of the samples. The melting peak temperature (T_m), the crystallization

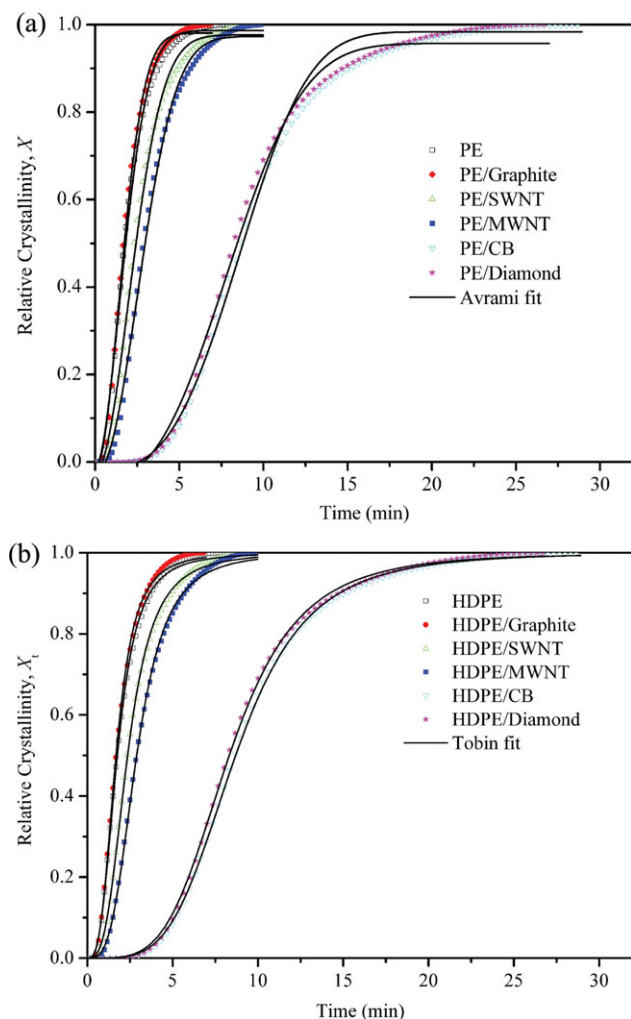


Figure 3. Fitting profiles of relative crystallinity curves for HDPE nanocomposites using (a) Avrami model and (b) Tobin model. T_c of 122°C is chosen for all the samples as an example. [Color figure can be viewed in the online issue, which is available at wileyonlinelibrary.com.]

peak temperature (T_c), the degree of supercooling (ΔT_c , defined as the difference between T_m and T_c),⁴¹ and the melting enthalpy (ΔH_m) were thus obtained. The absolute crystallinity of PE can be calculated by the following equation:

$$X_c = \Delta H_m / (w \Delta H_m^0) \quad (7)$$

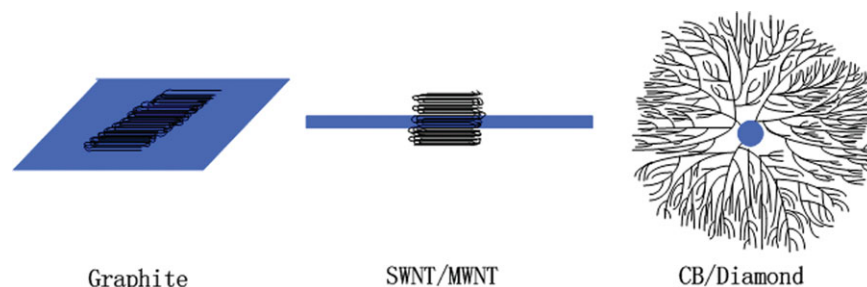


Figure 4. Schematic diagram of crystal growth of HDPE in the presence of various dimensional carbon nanofillers. [Color figure can be viewed in the online issue, which is available at wileyonlinelibrary.com.]

where $\Delta H_m^0 = 290$ J/g is the heat of fusion for PE with 100% crystallinity,^{42,43} and w is the weight fraction of PE in the composites. The values of T_m , T_c , ΔT_c , ΔH_m , and X_c are tabulated in Table III. There is no significant difference in ΔT_c between different samples. The crystallinity of HDPE exhibits a slight increase with the addition of graphite, SWNT or MWNT, whereas a slight decrease in crystallinity is observed with the addition of CB or diamond. Generally, with the nanofillers incorporated, the crystallinity of polymer can be either increased or decreased. On one hand, the carbon nanofillers could act as a nucleating agent resulting in an increased crystallinity. On the other hand, the nanofillers could also confine the crystallization since the crystallization of polymer could be restricted to a microenvironment surrounded by the nanofiller,⁴¹ which would lead to a decreased crystallinity. Hence, the decreased crystallinity of HDPE in the presence of CB or diamond might be due to the fact that the carbon nanofillers create a large interface between the PE molecules that surround the nanofillers. The interface region forms an amorphous phase, interferes with crystal growth and eventually limiting the overall degree of crystallinity.^{30,44} While, the slight increased crystallinity of HDPE with graphite, SWNT, or MWNT, could be attributed to the special structure of graphite sheet with continuum plane, which can easily absorb the HDPE chains and promote the crystallization along the surface, as presented in Figure 4.

The DSC curves of nonisothermal crystallization for HDPE and HDPE/carbon nanocomposites at different cooling rates (5, 10, 15, and 20°C/min) are shown in Figure 5. The nonisothermal crystallization parameters, such as the onset temperature of crystallization T_{onset} , the crystallization peak temperature T_c , and the enthalpy of crystallization ΔH_c have been determined from the DSC curves and the values are listed in Table IV. ΔH_c , T_{onset} , and T_{peak} all decrease with increasing cooling rate. At the high cooling rates, there was less time for the polymer chains to align themselves and hence, the crystallization was initiated at a later stage, leading to lower T_{onset} and T_{peak} . Meanwhile, the macromolecular chains do not have sufficient time to relax at the interface between amorphous and crystalline domain and thus, obtained a relatively low degree of crystallinity (corresponding to low ΔH_c).⁴⁴ For a given cooling rate, it is observed that the incorporation of SWNT, MWNT, CB, or diamond in HDPE leads to a successive decrease in T_{onset} and T_{peak} , while the presence of graphite does not cause significant change in T_{onset} and T_{peak} . The result is consistent with that of isothermal

Table III. The Crystallization and Melting Parameters of HDPE Extracted from Standard DSC Scans

Samples	T_c (°C)	T_m (°C)	ΔT_c (°C)	ΔH_m (J/g)	X_c (%)
HDPE	116.4	131.1	14.7	181.99	62.8
HDPE/Graphite	116.6	130.8	14.2	181.04	63.7
HDPE/SWNT	116.5	131.4	14.9	178.85	62.9
HDPE/MWNT	116.0	131.5	15.5	180.31	63.4
HDPE/CB	114.9	130.8	15.9	171.40	60.3
HDPE/ Diamond	115.2	130.8	15.6	176.63	62.1

crystallization studied above. With the addition of lower dimensional carbon nanofillers, the incubation time to reach the critical equilibrium nucleus dimension becomes longer and the molecular motion is retarded, thus T_{onset} and T_{peak} decrease. The unchanged T_{onset} and T_{peak} of HDPE/graphite nanocomposite are due to the nucleating effect of the incorporated graphite which exceeds the steric effects at the beginning of nonisothermal crystallization.

The X_t of nonisothermal crystallization can also be obtained by eq. (6). X_t of HDPE as a function of temperature is shown in Figure 6 as an example. The crystallization time t can be calculated by eq. (8):

$$t = \frac{T_{onset} - T}{\phi} \quad (8)$$

where T is the temperature at time t and Φ is the cooling rate. Thus, the half crystallization time $t_{1/2}$ for nonisothermal crystallization can also be obtained (Table IV). The half crystallization time $t_{1/2}$ of HDPE is in a descending order with the addition of 2-D, 1-D, and 0-D carbon nanofillers. The overall nonisothermal crystallization of HDPE is accelerated in the presence of 0-D carbon nanofillers and decelerated in the presence of 2-D

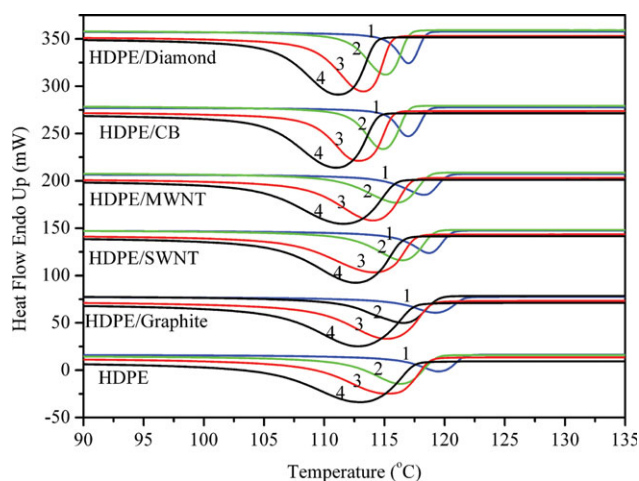


Figure 5. DSC curves of nonisothermal crystallization of HDPE and HDPE/carbon nanocomposites at different cooling rates: (1) 5°C/min, (2) 10°C/min, (3) 15°C/min, (4) 20°C/min. [Color figure can be viewed in the online issue, which is available at wileyonlinelibrary.com.]

Table IV. The Nonisothermal Parameters of HDPE Determined from DSC Exotherms

Samples	ϕ (°C/min)	T_{onset} (°C)	T_c (°C)	ΔH_c (J/g)	$t_{1/2}$ (min)
HDPE	5	123.8	119.5	195.16	1.15
	10	121.1	116.4	191.26	0.64
	15	120.5	115.3	190.86	0.49
	20	119.1	113.0	178.83	0.41
HDPE/Graphite	5	123.7	119.2	189.02	1.17
	10	122.0	116.6	188.96	0.72
	15	121.7	115.2	186.38	0.56
	20	120.2	112.9	174.67	0.47
HDPE/SWNT	5	122.5	118.7	184.38	1.03
	10	121.0	116.5	182.32	0.65
	15	119.6	114.2	180.28	0.50
	20	118.8	112.7	172.01	0.42
HDPE/MWNT	5	121.9	118.3	188.06	1.01
	10	120.5	116.0	190.81	0.61
	15	118.9	114.1	186.14	0.44
	20	117.5	112.2	174.07	0.39
HDPE/CB	5	119.9	117.0	183.81	0.71
	10	118.4	114.9	182.52	0.44
	15	117.0	112.9	181.92	0.35
	20	115.6	111.0	170.76	0.31
HDPE/Diamond	5	119.7	117.0	183.56	0.65
	10	118.5	115.2	183.30	0.45
	15	117.3	113.3	182.78	0.36
	20	115.6	111.1	170.99	0.30

graphite. The order of the nonisothermal crystallization rate is contrary to that of the isothermal crystallization rate, which can be discussed by the effects of the isothermal and nonisothermal process on the crystallization behavior. Generally, the

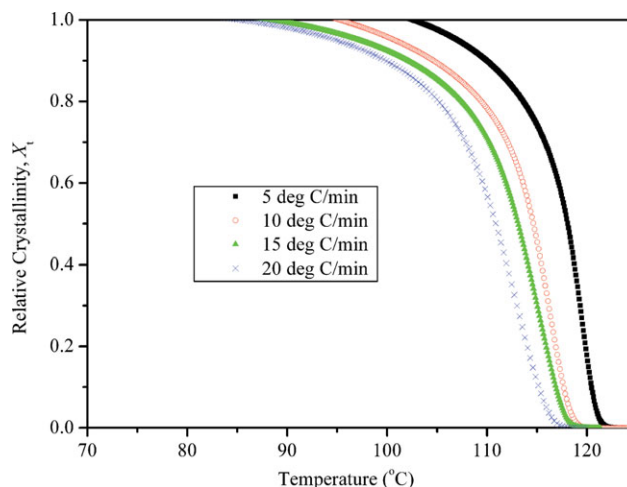


Figure 6. Development of relative crystallinity (X_t) with temperature for nonisothermal crystallization of HDPE. [Color figure can be viewed in the online issue, which is available at wileyonlinelibrary.com.]

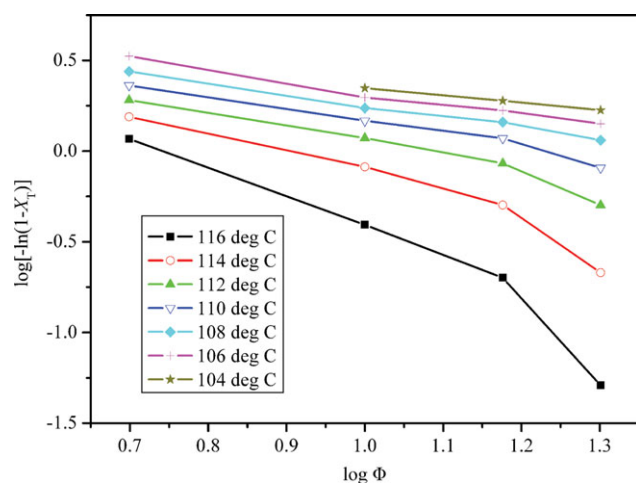


Figure 7. Ozawa plots for nonisothermal crystallization of HDPE. [Color figure can be viewed in the online issue, which is available at wileyonlinelibrary.com.]

crystallization rate is controlled by the nucleation and the crystal growth. For the isothermal study, as the crystallization was carried out under higher temperatures ($>120^{\circ}\text{C}$), the polymeric segments is flexible and can be easily transport to the growing crystal surface. Hence, the crystallization takes place by a nucleation-controlled mechanism, and the crystallization rate is mostly determined by the process of nucleation. Due to the nucleating effect of graphite, the isothermal crystallization of HDPE/graphite is thus accelerated. For the nonisothermal study, the crystallization was carried out under lower temperature (from 123°C to room temperature), in this situation, the crystal growth dominates the crystallization rate. The presence of nanofillers would hinder the crystal growth, the effect being more significant when the size of the nanofillers is larger. Hence, the crystallization rate of HDPE/graphite is the most hindered due to the largest dimension of the graphite. Besides the reasons mentioned above, it is worth noticing that, for a given cooling rate, the nonisothermal crystallization of HDPE/CB and HDPE/diamond nanocomposites takes place under a relatively low

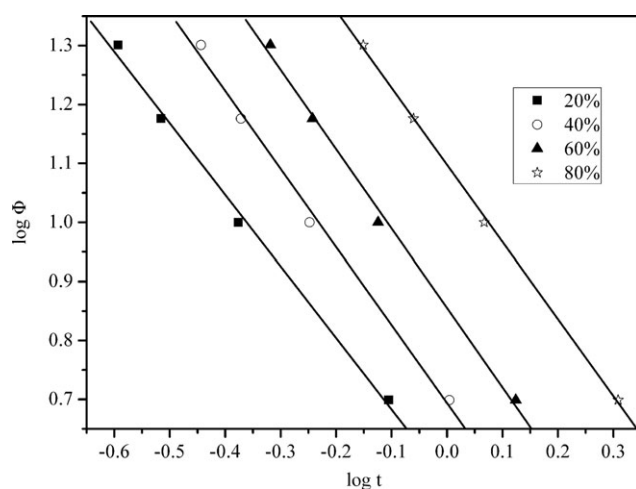


Figure 8. Plots of $\log \phi$ versus $\log t$ for HDPE.

temperature region in contrast to that of other samples. In the relatively low temperatures the crystallization is greatly accelerated (as revealed in the isothermal crystallization), thus the overall crystallization rate increases (i.e., $t_{1/2}$ decreases). While for HDPE/graphite, the situation is just the reverse leading to the lowest crystallization.

The Ozawa and Mo Methods. The nonisothermal crystallization behavior was analyzed by both Ozawa and Mo methods. The Ozawa plots of HDPE are shown in Figure 7 as an example. The Ozawa plots of pure HDPE and HDPE nanocomposites deviate from linearity when cooling rate varies from $5^{\circ}\text{C}/\text{min}$ to $20^{\circ}\text{C}/\text{min}$, which suggests that the Ozawa equation is not appropriate to describe the nonisothermal crystallization of HDPE and HDPE/carbon nanocomposites. The Ozawa method ignores the secondary crystallization and the dependence of fold length on crystallization temperature,⁴⁵ whereas for semicrystalline polymer like polyethylene, a large portion of crystallinity is attributed to the secondary crystallization.

The Mo model [eq. (5)] is hence used to analyze the nonisothermal crystallization behavior of HDPE. The relationships between $\log \phi$ and $\log t$ at different X_t for pure HDPE are show in Figure 8 as an example. The values of b and $F(T)$ for all the composites are listed in Table V. The small variation in the value of b for each sample and the clear linear relation between $\log \phi$ and $\log t$ indicate that the Mo method is applicable to describe the nonisothermal behavior of HDPE and HDPE/carbon nanocomposites. The values of b are comparable to those of PE/clay nanocomposite.⁴⁶ The value of $F(T)$ increases with increasing X_t for all the samples. At a given X_t , the values of $F(T)$ for HDPE/graphite nanocomposites are a bit higher than those obtained from pure HDPE. In contrast, the values of $F(T)$ for the nanocomposites with SWNT, MWNT, CB, and diamond are all lower than those for pure HDPE and are in a descending order. The lower values of $F(T)$ reflect that the corresponding nanocomposites can achieve the same degree of crystallinity faster than pure HDPE. The results imply faster kinetics of nonisothermal crystallization for HDPE in the presence of 1-D and

Table V. The Values of b and $F(T)$ versus Relative Crystallinity

X_t (%)		20	40	60	80
HDPE	B	1.21	1.32	1.34	1.31
	$F(T)$	3.64	4.94	7.16	12.52
HDPE/Graphite	B	1.50	1.51	1.49	1.44
	$F(T)$	3.52	5.22	7.73	13.66
HDPE/SWNT	B	1.39	1.48	1.47	1.30
	$F(T)$	3.14	4.36	6.70	12.95
HDPE/MWNT	B	1.32	1.39	1.39	1.37
	$F(T)$	2.98	4.18	6.15	11.08
HDPE/CB	B	1.44	1.61	1.75	1.56
	$F(T)$	1.78	2.31	3.20	7.81
HDPE/Diamond	B	1.59	1.73	1.85	1.82
	$F(T)$	1.47	2.02	2.94	7.10

0-D nanofillers, which are in agreement with the values of $t_{1/2}$ studied above.

Activation Energy. The activation energy ΔE for the transport of the macromolecular segments to the growing surface can be evaluated from Kissinger method:⁴⁷

$$\frac{d[\ln(\Phi/T_p^2)]}{d(1/T_p)} = \frac{-\Delta E}{R} \quad (9)$$

where R is the universal gas constant. The plots of $\ln(\phi/T_p)$ versus $1/T_p$ based on the Kissinger method are shown in Figure 9. The slopes of the lines drawn through these plots equal $-\Delta E/R$, and thus the activation energy ΔE can be determined. The results of ΔE are listed in Table VI. It is observed that the presence of carbon nanofillers in HDPE only cause a slight increase in the value of activation energy. The results suggest that the difference in crystallization kinetics of HDPE caused by various dimensional carbon nanofillers is largely related to the initiation of the nucleation process (including incubation and nucleation) rather than the growth process.

CONCLUSION

The influence of various carbon nanofillers on the isothermal and nonisothermal crystallization kinetics of HDPE was studied using DSC method. It was observed that carbon nanofillers with different dimensionality affect the crystallization behavior variously.

For isothermal studies at a given crystallization temperature, the crystallization rate of the nanocomposites follows the order: HDPE/2-D carbon > HDPE/1-D carbon > HDPE/0-D carbon, and the crystallization incubation time is in reverse order. The values of Avrami and Tobin exponents were obtained for the isothermal crystallization process. The process of crystal growth was two-dimensional heterogeneous in HDPE containing 1-D or 2-D carbon nanofillers and was three-dimensional heterogeneous in HDPE containing 0-D carbon nanofillers.

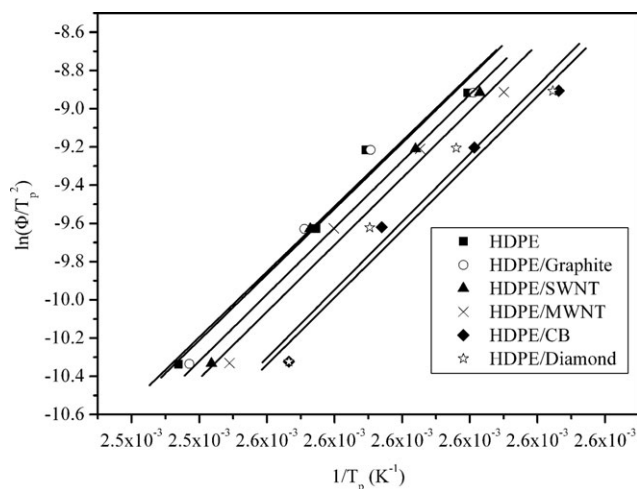


Figure 9. Kissinger plots of HDPE and HDPE/carbon nanocomposites.

Table VI. Activation Energy of HDPE and HDPE/Carbon Nanocomposites based on Kissinger Method

Material	$-\Delta E$ (kJ/mol)
HDPE	284.2
HDPE/Graphite	286.0
HDPE/SWNT	289.8
HDPE/MWNT	290.9
HDPE/CB	291.9
HDPE/Diamond	295.9

For nonisothermal studies, the overall rate of crystallization at a given cooling rate is in the order: HDPE/0-D carbon > HDPE/1-D carbon > HDPE/2-D carbon. The difference in the crystallization rate order between isothermal and the nonisothermal crystallization is caused by the difference in the crystallization mechanisms. The nonisothermal crystallization kinetics is investigated according to both Ozawa model and Mo model. Only the Mo method describes the nonisothermal crystallization behavior of HDPE and HDPE/carbon nanocomposites satisfactorily. The activation energy for the transport of crystalline units determined by Kissinger method does not vary much with the addition of carbon nanofillers.

ACKNOWLEDGMENTS

The authors are grateful to Prof. Siegfried Stapf for valuable discussion. This work is supported by National Natural Science Foundation of China (No. 21176208), National Basic Research Program of China (No. 2012CB720500), and the Fundamental Research Funds for the Central Universities (No. 2011QNA4032).

REFERENCES

- Alexandre, M.; Dubois, P. *Mater. Sci. Eng. R.* **2008**, *28*, 1.
- Homminga, D.; Goderis, B.; Dolbnya, I.; Groeninckx, G. *Polymer* **2006**, *47*, 1620.
- Homminga, D. S.; Goderis, B.; Mathot, V. B. F.; Groeninckx, G. *Polymer* **2006**, *47*, 1630.
- Huang, J. W. *J. Appl. Polym. Sci.* **2008**, *110*, 2195.
- Huang, J. W.; Hung, H. C.; Tseng, K. S.; Kang, C. C. *J. Appl. Polym. Sci.* **2006**, *100*, 1335.
- Liu, X.; He, A.; Du, K.; Han, C. C. *J. Appl. Polym. Sci.* **2011**, *119*, 162.
- Yuan, Q.; Awate, S.; Misra, R. D. K. *Eur. Polym. J.* **2006**, *42*, 1994.
- Yao, X.; Tian, X.; Zheng, K.; Zhang, X.; Zheng, J.; Wang, R.; Liu, C.; Li, Y.; Cui, P. *J. Macromol. Sci. Part B Phys.* **2009**, *48*, 537.
- Huang, J.-W. *J. Appl. Polym. Sci.* **2008**, *107*, 3163.
- Bal, S.; Samal, S. S. *Bull. Mater. Sci.* **2007**, *30*, 379.
- Dalmas, F.; Chazeau, L.; Gauthier, C.; Masenelli-Varlot, K.; Dendievel, R.; Cavaille, J. Y.; Forro, L. *J. Appl. Polym. Sci.* **2005**, *43*, 1186.

12. Coleman, J. N.; Khan, U.; Blau, W. J.; Gun'ko, Y. K. *Carbon* **2006**, *44*, 1624.
13. Shi, X. M.; Jiang, B. B.; Wang, J. D.; Yang, Y. R. *Carbon* **2012**, *50*, 1005.
14. Hu, Y.; Shenderova, O. A.; Hu, Z.; Padgett, C. W.; Brenner, D. W. *Rep. Prog. Phys.* **2006**, *69*, 1847.
15. Leelapornpisit, W.; Ton-That, M. T.; Perrin-Sarazin, F.; Cole, K. C.; Denault, J.; Simard, B. J. *Polym. Sci. Pol. Phys.* **2005**, *43*, 2445.
16. Valentini, L.; Biagiotti, J.; Lopez-Manchado, M. A.; Santucci, S.; Kenny, J. M. *Polym. Eng. Sci.* **2004**, *44*, 303.
17. Razavi-Nouri, M.; Ghorbanzadeh-Ahangari, M.; Fereidoon, A.; Jahanshahi, M. *Polym. Test* **2009**, *28*, 46.
18. Ahangari, M. G.; Fereidoon, A.; Kordani, N.; Garmabi, H. *Polym. Bull.* **2011**, *66*, 239.
19. Fereidoon, A.; Ahangari, M. G.; Saedodin, S. *Polym-Plast. Technol.* **2009**, *48*, 579.
20. Razavi-Nouri, M. *Iran. Polym. J.* **2009**, *18*, 167.
21. Haggmueller, R.; Fischer, J. E.; Winey, K. I. *Macromolecules* **2006**, *39*, 2964.
22. Trujillo, M.; Arnal, M. L.; Mueller, A. J.; Laredo, E.; Bredeau, S.; Bonduel, D.; Dubois, P. *Macromolecules* **2007**, *40*, 6268.
23. Vega, J. F.; Martinez-Salazar, J.; Trujillo, M.; Arnal, M. L.; Muller, A. J.; Bredeau, S.; Dubois, P. *Macromolecules* **2009**, *42*, 4719.
24. Zhou, Z.; Wang, S.; Lu, L.; Zhang, Y.; Zhang, Y. J. *Polym. Sci. Pol. Phys.* **2007**, *45*, 1616.
25. Soitong, T.; Pumchusak, J. *J. Mater. Sci.* **2011**, *46*, 1697.
26. Saeed, K.; Park, S.-Y. *J. Appl. Polym. Sci.* **2007**, *106*, 3729.
27. Zeng, H. L.; Gao, C.; Wang, Y. P.; Watts, P. C. P.; Kong, H.; Cui, X. W.; Yan, D. Y. *Polymer* **2006**, *47*, 113.
28. Jana, R. N.; Cho, J. W. *Compos. Part A.* **2010**, *41*, 1524.
29. Meng, H.; Sui, G.; Xie, G.; Yang, R. *J. Mater. Sci. Technol.* **2009**, *25*, 145.
30. Kim, J.; Kwak, S.; Hong, S. M.; Lee, J. R.; Takahara, A.; Seo, Y. *Macromolecules* **2010**, *43*, 10545.
31. Weng, W. G.; Chen, G. H.; Wu, D. J. *Polymer* **2003**, *44*, 8119.
32. Liu, Y.; Yang, G. *Thermochim. Acta.* **2010**, *500*, 13.
33. Causin, V.; Marega, C.; Marigo, A.; Ferrara, G.; Ferraro, A. *Eur. Polym. J.* **2006**, *42*, 3153.
34. Avrami, M. *J. Chem. Phys.* **1939**, *7*, 1103.
35. Avrami, M. *J. Chem. Phys.* **1940**, *8*, 212.
36. Tobin, M. C. *J. Polym. Sci. Pol. Phys.* **1974**, *12*, 399.
37. Ozawa, T. *Polymer* **1971**, *12*, 150.
38. Evans, U. R. *Trans. Faraday. Soc.* **1945**, *41*, 365.
39. Liu, T. X.; Mo, Z. S.; Wang, S. G.; Zhang, H. F. *Polym. Eng. Sci.* **1997**, *37*, 568.
40. Long, Y.; Shanks, R. A.; Stachurski, Z. H. *Prog. Polym. Sci.* **1995**, *20*, 651.
41. He, L. H.; Xu, Q.; Song, R.; Hui, C. W. *Polym. Compos.* **2010**, *31*, 913.
42. Abbasi, S. H.; Hussein, I. A.; Parvez, M. A. *J. Appl. Polym. Sci.* **2011**, *119*, 290.
43. Bensason, S.; Minick, J.; Moet, A.; Chum, S.; Hiltner, A.; Baer, E. *J. Polym. Sci. Pol. Phys.* **1996**, *34*, 1301.
44. Adhikari, A. R.; Lozano, K.; Chipara, M. *J. Compos. Mater.* **2012**, *46*, 823.
45. Joshi, A.; Butola, B. S. *Polymer* **2004**, *45*, 4953.
46. Yuan, Q.; Awate, S.; Misra, R. D. K. *J. Appl. Polym. Sci.* **2006**, *102*, 3809.
47. Kissinger, H. E. *J. Res. Natl. Bur. Stand.* **1956**, *57*, 217.